





Article

Computer-Aided Surgical Simulation through Digital Dynamic 3D Skeletal Segments for Correcting Torsional Deformities of the Lower Limbs in Children with Cerebral Palsy

Leonardo Frizziero ¹, Giovanni Trisolino ^{2,*}, Gian Maria Santi ¹, Giulia Alessandri ¹, Simone Agazzani ¹, Alfredo Liverani ¹, Grazia Chiara Menozzi ², Giovanni Luigi Di Gennaro ², Giuseppina Maria Grazia Farella ³, Alida Abbruzzese ³, Paolo Spinnato ⁴, Lisa Berti ³ and Maria Grazia Benedetti ³

¹ Department of Industrial Engineering, Alma Mater Studiorum University of Bologna, 40136 Bologna, Italy

² Paediatric Orthopaedics and Traumatology, IRCSS—Istituto Ortopedico Rizzoli, 40136 Bologna, Italy

³ Physical Medicine and Rehabilitation Unit, IRCSS—Istituto Ortopedico Rizzoli, 40136 Bologna, Italy

⁴ Diagnostic and Interventional Radiology, IRCSS—Istituto Ortopedico Rizzoli, 40136 Bologna, Italy

* Correspondence: giovanni.trisolino@ior.it; Tel.: +39-051-636-6484



Citation: Frizziero, L.; Trisolino, G.; Santi, G.M.; Alessandri, G.; Agazzani, S.; Liverani, A.; Menozzi, G.C.; Di Gennaro, G.L.; Farella, G.M.G.; Abbruzzese, A.; et al. Computer-Aided Surgical Simulation through Digital Dynamic 3D Skeletal Segments for Correcting Torsional Deformities of the Lower Limbs in Children with Cerebral Palsy. *Appl. Sci.* **2022**, *12*, 7918. <https://doi.org/10.3390/app12157918>

Academic Editors: Peter Kokol and Oludayo Olugbara

Received: 19 July 2022

Accepted: 5 August 2022

Published: 7 August 2022

Publisher's Note: MDPI stays neutral with regard to jurisdictional claims in published maps and institutional affiliations.



Copyright: © 2022 by the authors. Licensee MDPI, Basel, Switzerland. This article is an open access article distributed under the terms and conditions of the Creative Commons Attribution (CC BY) license (<https://creativecommons.org/licenses/by/4.0/>).

Abstract: Torsional deformities of the lower limb are common in children with cerebral palsy (CP)-determining gait problems. The mechanisms underlying transverse plane gait deviations arise from a combination of dynamic and static factors. The dynamic elements may be due to spasticity, contractures and muscle imbalances, while the static ones may result from excessive femoral anteversion, which decreases the efficiency of the hip abductors by reducing the muscular lever arms. A therapeutic approach has been identified in multi-level functional surgery for the lower limb. Treating the malalignments of the lower limb with femoral or tibial derotation provides optimal results, especially when supported by adequate biomechanical planning. This planning requires an integrated static-dynamic approach of morphological and functional evaluation, based on radiological measurements, physical examination and gait analysis. Instrumented gait analysis has been confirmed as essential in the evaluation and surgical decision making process for children affected by CP with transverse plane deformities. Computational simulations based on musculoskeletal models that integrate patient-specific CT morphological data into gait analysis can be used for the implementation of a surgical simulation system in pre-operative planning to test the possible effects of the different surgical treatment options on the torsional defects of the lower limbs. Recently, a computer-aided simulation process has been implemented in the preoperative planning of complex osteotomies for limb deformities in children. Three-dimensional (3D) digital models were generated from Computed Tomography (CT) scans, using free open-source software. The aim of this study is to integrate the patient-specific CT musculoskeletal model with morphological data and gait analysis data, with the personalized calculation of kinematic and kinetic parameters, which allow us to generate an “avatar” of the patient for a more in-depth evaluation of the gait abnormalities. The computational simulation platform proposed provides a realistic movable musculoskeletal model in a virtual environment, with the possibility of planning and monitoring the effects of virtual three-dimensional surgical corrections.

Keywords: cerebral palsy; torsional deformities; derotation; musculoskeletal modeling; virtual surgical planning; avatar; gait analysis; computed tomography

1. Introduction

Torsional deformities of the lower limbs, such as femoral neck anteversion and tibial torsion, are frequent in children with infantile cerebral palsy (CP) [1]. These alterations cause important functional problems in walking, also related to the internal deviation of the angle of progression of the foot, with an increased risk of falls, pain, overloading and muscle fatigue [2,3]. The mechanisms underlying transverse plane gait deviations arise

from a combination of dynamic and static factors. The dynamic elements may be due to spasticity, contractures and muscles imbalance, while the static ones may result from excessive femoral neck anteversion which decreases the efficiency of the hip abductors by reducing the muscular lever arms [4]. The orthopedic therapeutic approach has been identified in multi-level functional surgery for the lower limbs, which can include the simultaneous correction of static and dynamic factors [5,6]. Single-event multi-level functional surgery (SEMLS) has shown favorable effects on the clinical and functional parameters of children suffering from CP with torsional alterations of the lower limbs [7,8]. In particular, the combination of soft tissue surgery and bony procedures such as derotation osteotomies is providing promising results [9,10], especially when supported by adequate biomechanical planning [11,12]. This planning requires an integrated static-dynamic approach of morphological and functional evaluation, based on radiological measurements, physical examination, and instrumented gait analysis [13–15]. The accuracy of the measurement of anatomical parameters by imaging (MRI and CT) is essential for the design of the femoral and/or tibial derotation surgery [16]. Instrumented gait analysis has been confirmed as essential in patient assessment and surgical decision making for children affected by CP with transverse plane deformities [17,18]. Gait analysis combined with clinical evaluation can influence the planning of functional surgery, and also improves the outcomes for patients undergoing the procedures themselves [19,20]. A recent meta-analysis confirmed the positive effects of femoral derotational osteotomy on the kinematics of pelvis and hip in the transverse plane [21]. However, dynamic hip rotation cannot be predicted exclusively by physical examination measures of hip range of motion or from three-dimensional assessment of femoral neck anteversion derived from biplanar radiographs [22]. The combination of morphological data from imaging and functional data from instrumented gait analysis has been revealed to be the most reliable method for supporting surgical decision making. Computational simulations based on musculoskeletal models that integrate patient-specific MR/CT morphological data into gait analysis [23–26] allow more reliable calculations of kinematic and kinetic parameters. This modelling can also be used for the implementation of a surgical simulation system in pre-operative planning to test the possible effects of the different surgical treatment options in torsional defects of the lower limbs [27,28]. The digital 3D models obtained from CT scans have been already used for surgical planning in a selected group of pediatric patients suffering from complex multiplanar limb deformities [29]. The implementation of the surgical decision making process, using both a morphological and functional evaluation approach, aims to improve the outcomes of the interventions. The integration of this information into surgical decision making may be useful to optimizing performance of techniques and avoiding pitfalls and complications.

The aim of this study is the creation of a patient-specific musculoskeletal model that integrates patient-specific CT morphological data and gait analysis with personalized calculation of kinematic and kinetic parameters. A computational simulation platform is proposed for obtaining a realistic movable musculoskeletal model in a virtual environment, with the possibility of planning and monitoring the effects of virtual three-dimensional surgical corrections.

2. Materials and Methods

The study was pilot research investigating the feasibility of a novel computational process for obtaining a realistic movable musculoskeletal model in virtual environment. This model integrated patient-specific CT morphological data into gait analysis, with personalized calculation of kinematic and kinetic parameters. The present model was compared with a standard model [30] and provided a computational simulation platform for virtual three-dimensional surgical planning. The process consists of the following steps, outlined in Figure 1.

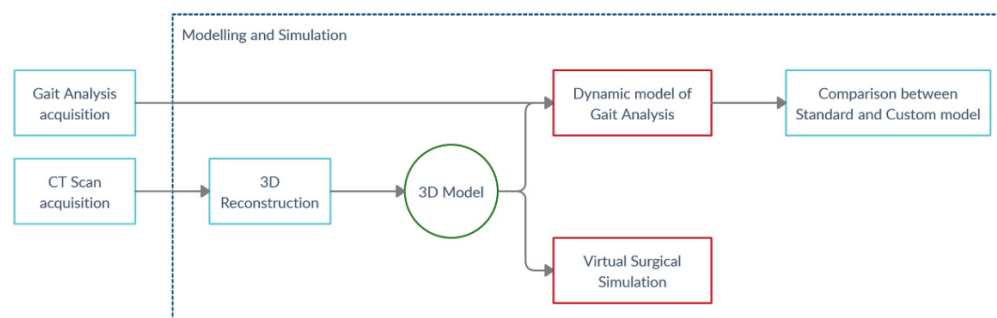


Figure 1. Methodology workflow.

As an example, here is a case description of a 13-year-old adolescent with a complex pattern of crouch gait, valgus knee and intoeing due to cerebral palsy, GMFCS 2.

2.1. Gait Analysis Acquisition

The patient underwent state-of-the-art gait analysis (GA). Five trials of barefoot level walking at a self-selected speed on a 10 m walkway were recorded. An additional static trial was recorded in standing upright position. The patient was instrumented with reflective markers on the pelvis and lower limbs according to an established marker-set and protocol [31–33]. Three-dimensional marker trajectories were collected using an eight-camera motion capture system [100 Hz, Vicon 612 Motion System, Oxford (UK)]. By still wearing the GA markers, patients received full lower-limb CT. The information was exported in C3D format.

2.2. CT Scan Protocol

Computed tomography (CT) studies of the lower limbs were acquired with a low-dose protocol, using a full iterative reconstruction model-based (MBIR) algorithm (VEO) [34]. A VEO algorithm has been introduced in current clinical practice at our institute, having demonstrated a significant decrease in radiation dose in children [35]. CT studies were acquired, including of the entire lower limbs (from the iliac wings to the whole feet), with a volumetric acquisition protocol optimized using a slice thickening of 5 mm (0.625 mm reconstructions) [CT Equipment: Discovery Dual Energy 256 Slices, General Electric (GE), Boston, Massachusetts (USA)]. The radiation dose length product (DLP) was 70 mGy/cm with an estimated effective dose to the patient of about 0.5 mSv. Before the CT acquisitions, the 22 reflective markers were secured to anatomic locations with double-sided adhesive tape on the skin, and successively included in the CT field of view. Post-processing reconstructions with images superimposition were performed to calculate femoral anteversion and external tibial torsion angles which resulted in the following readings: external tibial torsion (ETT) 28° right, 29° left; femoral neck anteversion (FNA) 38° right, 39° left. Femoral length were found to be 39.25 mm at the right side, and 39.25 mm at the left side; tibial length was 31.22 mm at the right side, and 31.23 mm at the left side. All acquisitions were exported in DICOM format.

2.3. Modelling and Simulation Workflow

The skeletal reconstruction process was followed according to a method already used in our unit. Briefly, this methodology consists of CT image acquisition and reprocessing and 3D model reconstruction [29,36].

3. Results

3.1. 3D Reconstruction of Patient-Specific CT Scan

Figure 2 shows in detail the steps for reconstructing the 3D model from the CT scan.

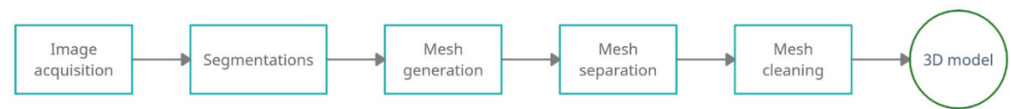


Figure 2. 3D Modelling workflow.

First, the DICOM file was imported in 3DSlicer [37], a software to read and process the CT scan, that is widely used for medical, biomedical, and imaging research. In this environment, the medical images were manipulated, by adjusting their brightness and contrast so that the visibility of the affected part is highlighted. In this case, it was important to bring out both the bone tissue and the markers. Brightness and contrast are adjusted by two values, the level value and the window weight value, respectively. The level corresponds to the average brightness level of the pixels on the monitor. Increasing the level makes the image darker; decreasing the level value makes the image brighter. The window width determines the range of pixel values that will be incorporated into the display. Increasing window weight reduces the contrast of the display, while decreasing window weight increases the brightness range between two consecutive pixel values. Once the correct visualization was set up, the selection of the relevant part was made using segmentation. It is possible to create selection according to the desired tissue, capturing only the anatomical parts of interest. A series of tools was used to capture a defined range of pixel intensity. The resulting model integrated both bones and external markers, distinguished by two selection masks (Figure 3).

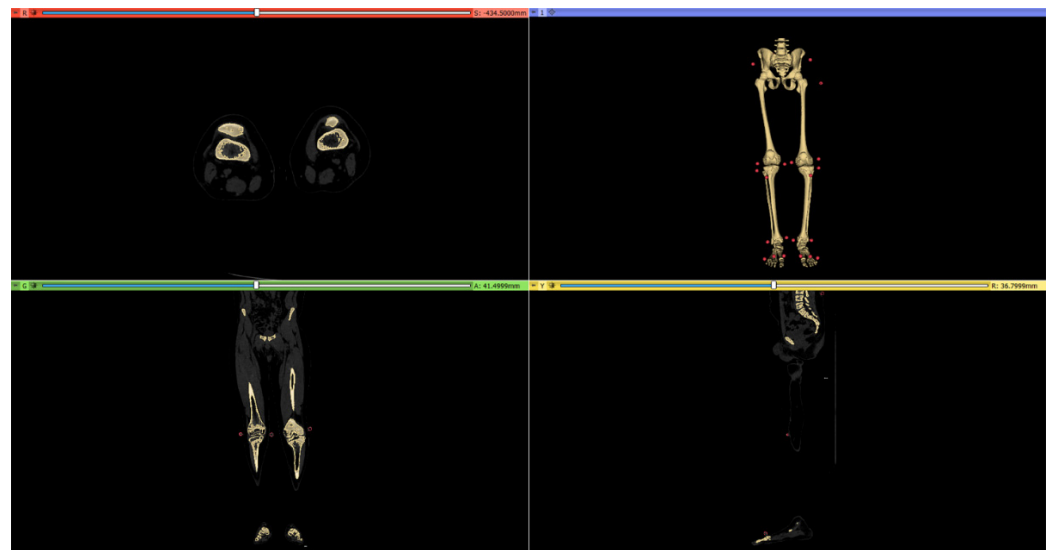


Figure 3. CT scan reconstruction using 3DSlicer. The brightness was set to 400 and contrast to 1000. For bone tissue reconstruction was selected a range of pixel intensity between 150 and 3264, while for the markers a range between 250 and 3264.

Since this model could not be used directly in motion and virtual simulation software, as all anatomical components were part of a single “.stl” file, it was necessary to import the “.stl” file into the modelling software, Blender v2.93 [38]. In this environment each bone was selected and separated from the others (Figure 4). The result was composed by twelve three-dimensional models of each anatomical part, from the pelvis to the feet, and a three-dimensional model of the markers.

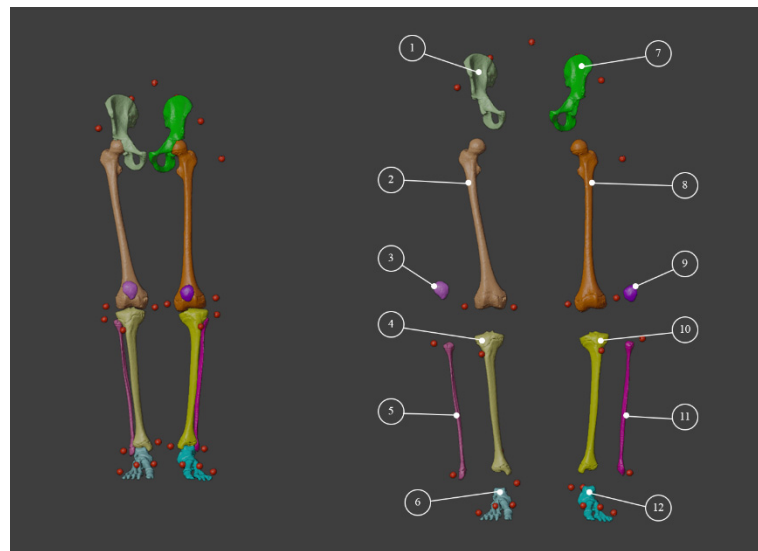


Figure 4. Bone separation using Blender.

Then, the separated files were lightened and cleaned up using MeshLab v2021.07 [39] by applying the “Ambient Occlusion” filter and selecting unsuitable vertices. This step was necessary to remove unnecessary internal parts and have a surface model. The model prepared in this way can be used for simulation processes [36,40].

3.2. Dynamic Model of Patient-Specific Gait Analysis

The software used to build the patient model was NmsBuilder v2.1 [41], which is a freeware software used to perform the pre-processing of musculoskeletal modelling. It allowed us to create a model in an OpenSim environment, starting from three-dimensional “.stl” geometries. NmsBuilder can import different types of biomedical data, display it interactively, merge it into a comprehensible representation, as well as manipulating reference points, surfaces and volumes, while defining and calculating musculoskeletal parameters. In particular, the process used to obtain the movable skeletal model was the following:

1. Importation of the model in “.stl” format (including the markers) into the NmsBuilder;
2. Identification of the names of the markers associated with the stereophotogrammetry files and their position in the model;
3. Creation of the necessary anatomical markers directly suggested by the software;
4. Use of the newly created markers to create the reference systems for the joints;
5. Creation of the OpenSim model.

The entire process is outlined in the block diagram of Figure 5.

The geometries were imported into NmsBuilder and the virtual markers were manually positioned to match the real markers from the CT data as seen in Figure 6.

Having completed these steps, the model markers were created manually using the “Create anatomical landmark cloud” command. This command allowed us to automatically identify the names of the markers necessary for a correct construction of the model. Placement of markers was found in literature to be usually performed through comparison and study of the spatial location of the markers; in this case instead, it was possible to position the markers directly on the geometries of the CT scan (Figure 7), superimposing the spheres generated by NmsBuilder on them. After the positioning step, the markers were used to create the reference systems of the joints, which are positioned autonomously (command: “Create anatomical reference system”) for all the bone geometries.

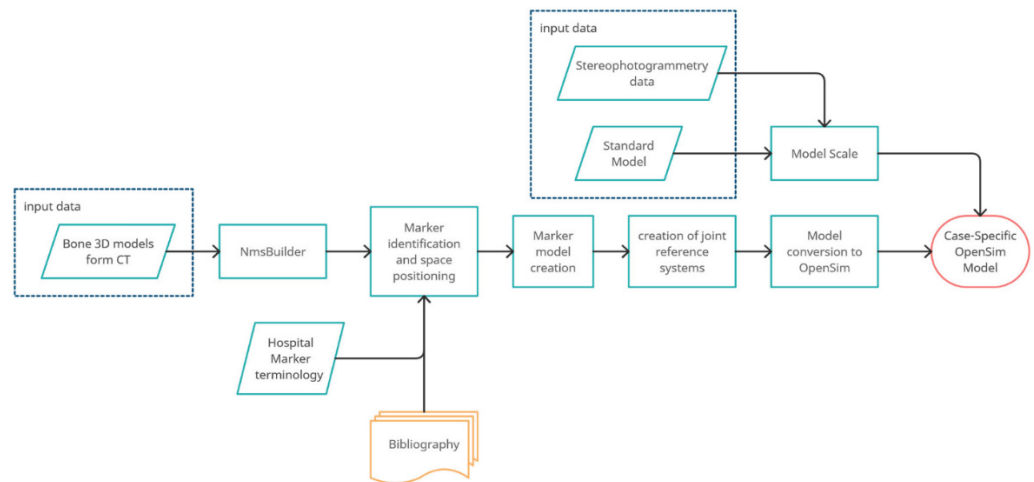


Figure 5. Flowchart describing the creation of OpenSim model using NmsBuilder and 3D TC models.

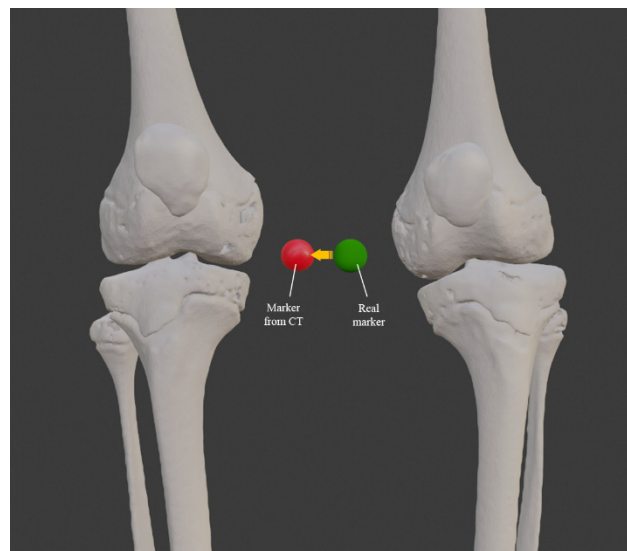


Figure 6. On the right the marker from the associated model, on the left the marker from CT not yet associated.

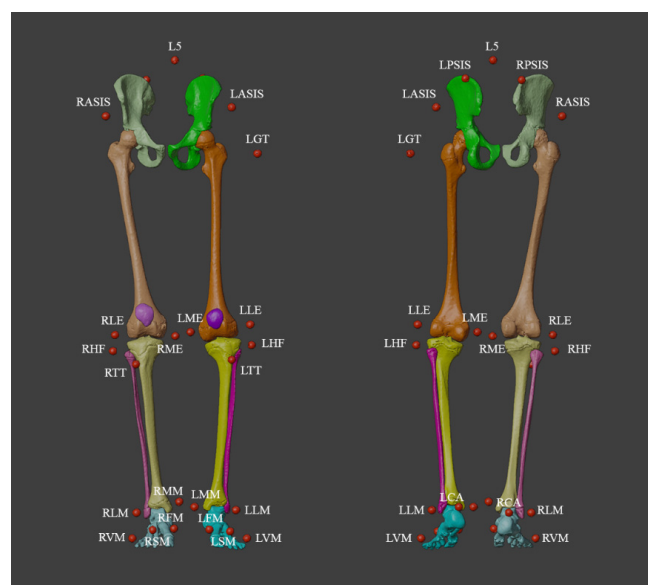


Figure 7. Anatomical landmark system.

This command generated two reference systems, one considered as father and the other considered as child; these must be associated respectively with the bones of the analyzed joint; for example, with the knee joint the femur will be considered as a father and the tibia as a child. Furthermore, it was necessary in order to create the patient's customized model, to convert the file into an OpenSim file. To reach this purpose, the software has a series of commands available such as: "create body", "create free joint to the ground", "create joint", "create marker set", create "wrap object", create "muscle". Specifically, these commands created the virtual bones of the model. To create the ground joint needed to support the skeleton in the OpenSim environment, it was necessary to create the joints of the model and associate each bone model with its relative markers. The "wrap object" and "muscle" commands allowed us to create surfaces on which the muscles could be bent in the most natural and realistic way possible. Using these commands, it was possible to obtain the subject specific model used for the study.

3.3. Comparison between Standard and Custom Model

The specific model of the patient was then compared with a standard model [30], which has a greater level of detail at the articulation level. It also presented a schematization of the human muscular system that would require more data with respect to the CT scan, in order to determine the insertion points of each individual muscles. For this reason, it tends to be carried out only when it is actually necessary. To compare the two models (standard and custom) it was necessary to adapt the standard model to the case study by unifying the marker nomenclature. Subsequently, the scaling phase of the standard model was carried out, which was the operation by which it was possible to make the standard model coincide with the markers relating to the analysis of the patient's movement. An effective scaling of the model was usually considered to be when the error was less than 20 mm. Six Gait Analyses (Gait_0, Gait_1, Gait_2, Gait_3, Gait_4, Gait_5) were analysed for the case study. As described in Figure 8, two Gait Analyses were required to obtain a standard model that represented the patient's movement. In particular, Gait_0 (Dynamic analysis) and Gait_5 (static analysis) were used to rescale the standard model. To resize a model, it was necessary to collect data from the subject in a static pose (Gait_5), measure the subject's specifications and related body segments also using the position of the markers and add the functional joint centres from a dynamic test (Gait_0). Because they were used for calibration, these two gait analyses were not considered for the following comparison. Gait_2 and Gait_4 were discarded because they presented problems in marker definition. Finally, Gait_1 and Gait_3 were the two gait analyses used to study the motions applied both to the standard and patient-specific models.

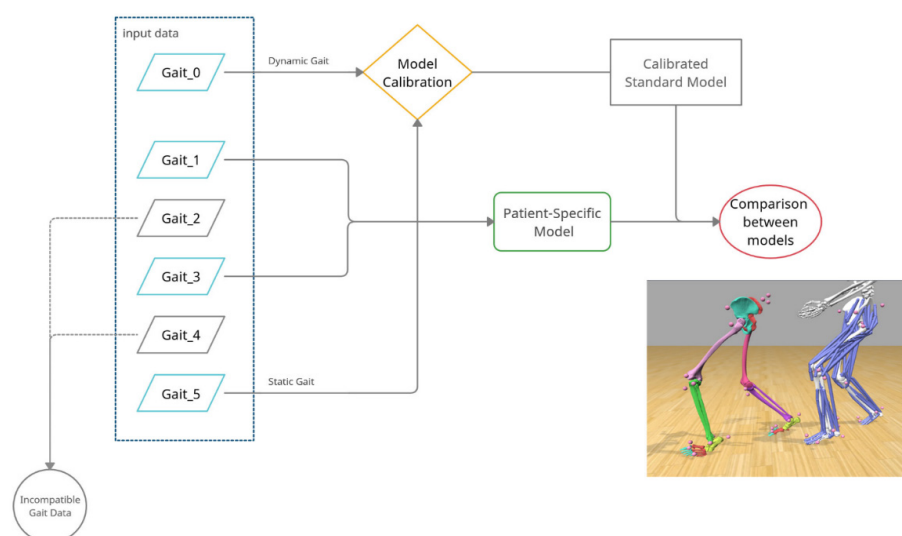


Figure 8. Flowchart of comparison between standard and custom model.

Once an adequate standard model scaling was obtained, the two models were compared by performing the inverse kinematics on the movement data obtained by stereophotogrammetry. For comparison, the following error parameters provided for each frame:

- Total Square Error (TSE)
- Root Mean Square Error (RMSE)
- Maximum Error (ME).

Tables 1 and 2 contain the mean, maximum value and standard deviation as a function of each motion analysis.

Table 1. Mean, Maximum value and Standard Deviation in Gait 1.

Gait 1								
Standard Model			Patient-Specific Model				Comparison	
	AVERAGE (mm)	MAX (mm)	STANDARD DEV (mm)	AVERAGE (mm)	MAX (mm)	STANDARD DEV (mm)	VARIATION MAX ERROR (%)	VARIATION STD DEV (%)
TSE	5.2	9.7	1.6	5.6	7.1	0.6	26.6	59.2
RMSE	14.0	19.3	2.1	15.0	16.9	0.8	12.6	58.9
Max Error	30.6	41.8	5.4	27.8	33.7	2.1	19.3	61.1

Table 2. Mean, Maximum value and Standard Deviation in Gait 3.

Gait 3								
Standard Model			Patient-Specific Model				Comparison	
	AVERAGE (mm)	MAX (mm)	STANDARD DEV (mm)	AVERAGE (mm)	MAX (mm)	STANDARD DEV (mm)	VARIATION MAX ERROR (%)	VARIATION STD DEV (%)
TSE	4.9	9.1	1.4	5.9	7.6	0.8	16.9	43.4
RMS	13.6	18.7	1.8	15.3	17.4	1.0	7.0	45.3
Max Error	28.4	40.3	5.6	28.6	34.0	2.0	15.4	64.6

The software reported the Total Square Error for the worst markers of each frame analysed. The average value, the maximum value and the standard deviation were calculated in order to understand the trend of the markers that were less adherent to the gait analysis for each type of error, both for the Standard model and the Patient-Specific model. Finally, the variation between maximum errors and standard deviation in all three errors were calculated. It could be observed that the patient-specific model had a maximum error that spanned from 12.6% to 26.6% less than the maximum error of the standard model for Gait_1, and was between 7% and 15% less for Gait_3. Concerning standard deviations, it was observed that for both cases, the patient-specific model has half the values of the standard model. In conclusion, from the comparison of the two models, it was found that the customized model was the one that usually had the lowest maximum error and that it was more constant having a usually lower standard deviation, making it preferable to the scaling of the standard model. Moreover, the customized model took into account possible bone deformities or joint placements that the standard model did not consider.

3.4. Virtual Surgical Simulation

The 3D model was then used for simulating the effects of surgical correction. In Blender it is possible to simulate the cut of the bones, displaying in a three-dimensional fashion the effects of osteotomies. In particular, in this case, a double level osteotomy was planned and simulated for the left leg. The first osteotomy was a closed wedge extension osteotomy for compensating 20° knee flexion (Figures 9 and 10).

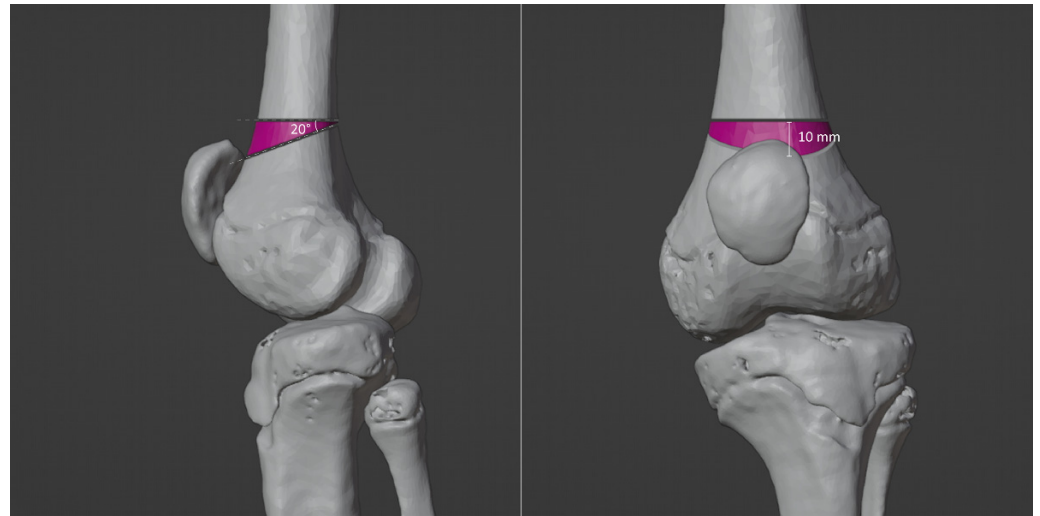


Figure 9. Closed wedge simulation. The left femur had to be corrected by 20° in extension.

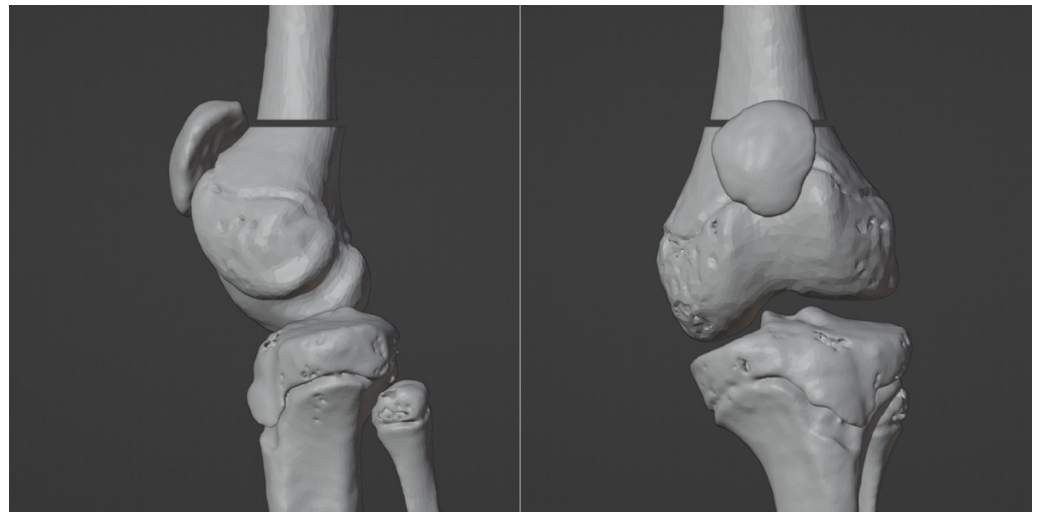


Figure 10. Femoral extension simulation.

This osteotomy was also combined with a femoral derotation for compensating excessive femoral anteversion (Figure 11). The second osteotomy, a pure rotational osteotomy of the distal tibia and fibula, was also simulated for correcting residual excessive tibial external torsion (Figure 12). The planned surgery was successfully performed by using patient specific instrumentation (Figure 13).

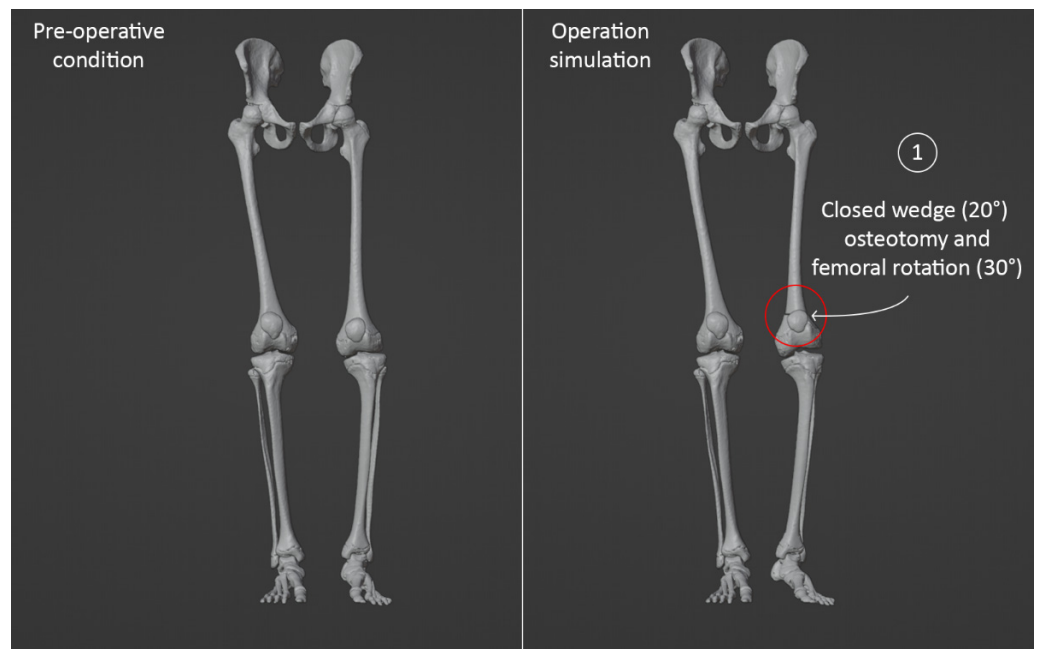


Figure 11. Comparison between the baseline appearance of the 3D model and the same model after simulating the femoral extension-derotation osteotomy. The patella is pointing forward, but the foot is pointing outward.

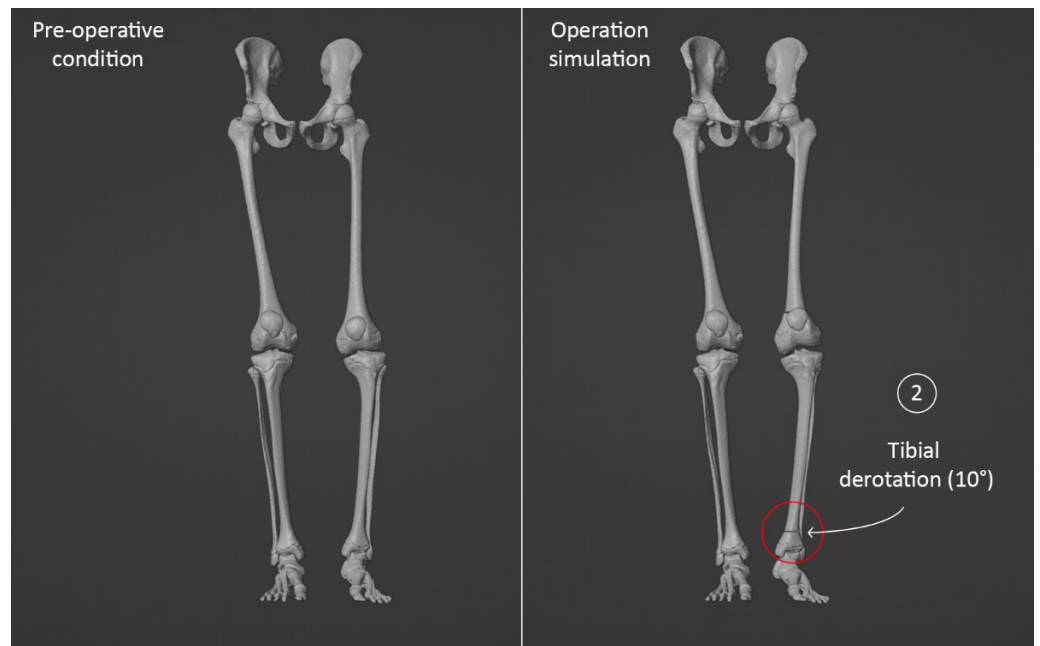


Figure 12. Comparison between the baseline appearance of the 3D model and the same model after both femoral and tibial osteotomies, showing that the patella and foot are pointing forward.



Figure 13. Preoperative and postoperative radiographs.

4. Discussion

CP is the most common cause of aberrant gait pattern and physical disability in children. The neurological impairment leads to progressive musculoskeletal pathology with muscle-tendon contractures, secondary progressive bony deformities and joint instability. Orthopedic procedures have been designed to address the various components of the progressive musculoskeletal pathology including tendon lengthening, tendon transfers, rotational osteotomies, and joint stabilization procedures. However, planning the surgical strategy in SEMLS is often difficult and no obvious prediction can be made about the effects of surgery on the gait pattern. Currently, the surgical planning of such complex cases is generally accomplished on the basis of the clinical examination and plain radiographs. CT scans are rarely required only to investigate potential torsional deformities.

Gait analysis has demonstrated to improve the decision making and possibly alter the surgical indication, but it requires extensive learning curve and experience from surgeons for a correct interpretation of data.

This study presents an integrative framework for obtaining a “virtual movable musculoskeletal model” of the lower limbs. This virtual musculoskeletal model is obtained by linking data from gait analysis and a CT-based subject-specific model of the lower limbs. The main finding of our study was that it is possible to use our proposed technique in clinical practice as the gait analysis is a non-invasive examination, the software used in our methods are freely available and low-dose CT scans of the lower extremities are possible [42]. The possibility of obtaining a musculoskeletal model of the patient, capable of combining patient-derived anatomic models and data from gait analysis, is the key factor for improving our understanding of such complex pathology. Throughout computer-aided surgical simulation it is possible to predict the effect of surgery on gait pattern, especially when combined and multilevel procedures are planned in a single event operation [43–45].

In this context, the creation of virtual movable skeletal models, based on the specific patient anatomy, is an appealing option for several purposes, especially for virtual surgical

planning and simulation. The main advantages of subject-specific models have been already reported by some authors [26,46]. Scheys and colleagues analyzed six children with aberrant gait and torsional deformities of the lower limbs due to CP. They reported that patient-specific MR-based models were more accurate in estimating moment arm length compared to rescaled generic models, confirming that inter-individual variation in musculoskeletal geometry, such as muscle attachment locations and femoral anteversion, play a crucial role in the accuracy of moment arm length calculations [26].

We used CT scans for modeling the skeleton of the lower limbs, applying a very low-dose protocol (VEO, General Electrics). We performed a volumetric-spiral CT acquisition that permits high quality and detailed 2D and 3D imaging reconstructions. This technique offers higher imaging details than EOS. Of course, the effective estimated radiation dose to the patient with this acquisition is significantly lower than a standard CT acquisition (at least 70–80% dose reduction), even if higher than the effective dose obtained with EOS. In this acquisition, the inclusion of iliac wings was required, and this led to an increase of the effective estimated dose to the patient, due to the inclusion of the pelvis in the scanned volume. In protocols performed in lower limbs only, with this low-dose CT technique, the effective dose to the patient (mSv) would dramatically decrease. The main advantage of this method is the possibility of obtaining very accurate volumetric reconstructions of the bone (and possibly of the soft tissues), even including the reflective markers in the field of view. Further methods have been described for obtaining 3D models to obtain 3D models of the lower limbs. Low-dose simultaneous perpendicular biplanar radiography with secondary 3D reconstruction (EOS) is an appealing alternative option to CT, but relies on the correct identification of bony landmarks; this can be hard to identify in the immature skeleton, potentially hampering the torsion measurements in children [47–49].

Moreover, recent advancements in MRI techniques allow us to obtain high quality reconstructions, with almost similar details compared to the reconstructions based on CT. Particularly, isotropic 3D MRI provide higher resolution quality images than standard 2D sequences, leading to a reduction in artifacts and allowing multiplanar reconstructions [50]. Anyway, the reflective elements placed on the skin, such as in this case, must be MRI-compatible, and their morphology must be accurately planned to fit in the MRI coil. Moreover, MRI has higher acquisition time and lower tolerance, especially among pediatric patients that may require sedation or anesthesia during the exams.

Another advantage of our computational integrative framework is that it was implemented using as a set of open-source software, thus potentially improving the cost-effectiveness ratio. To date, several freely available software for modeling and simulation of both musculoskeletal and FE models exists [51,52]. Nonetheless, the verifications of the models, the validations and the sensitivity studies, are still challenging mainly because the biomechanical community has not reached a complete consensus on many points (e.g., the software used for modeling and simulating in a biomechanical framework) [46].

The present study must be considered in light of some limitations. The surface reflectors are not exactly sure to reproduce the patient's muscle movements. The procedure is still very laborious and requires a long time to create one or more models and a highly skilled staff. Machine learning processes will be able to overcome these timescales. Using a trained neural network with a database of solved gait analysis cases and 3D reconstructions would be possible to build an algorithm that facilitates the construction of the patient-specific models. Specifically, starting from the input of the CT scan and gait analysis it would be possible to have as output the automatic reconstruction and perfectly posed 3D model. Unfortunately, there is not much data available since these cases are uncommon. In addition, the simultaneous arrangement of CT and gait analysis is not obvious. Therefore, the construction of an organized database for training neural networks could be envisaged before the usage of the algorithm itself.

The virtual surgical planning has not so far evaluated the effect of soft tissue procedures, such as patellar tendon plication or hamstrings lengthening, that should be combined with the bony procedures. Finally, there is no counterevidence that the simulations carried

out are valid since the current research protocol does not allow us to execute postoperative CT in children simply for research purposes. Many cases would be needed to ascertain the accuracy of the analysis process.

Regardless of these limitations and with these ideas in mind, we have presented an integrative framework of “virtual movable musculoskeletal model” of the lower limbs. We have understood virtual movable musculoskeletal models as “musculoskeletal avatar” of the patient, having several applications beyond virtual surgical planning, from rehabilitation to telemedicine, from education to robotic surgery. Work is ongoing for using both 3D reconstructions of the skeleton and muscles, in different cases of children with and without CP, in order to predict the post-operative gait pattern, also combining bony and soft tissues multilevel procedures.

Author Contributions: Conceptualization, L.F., G.T., A.L. and M.G.B.; methodology, G.M.S., G.A. and S.A.; software, G.M.S.; validation, G.M.G.F. and A.A.; formal analysis, G.M.S.; investigation, L.B., P.S. and G.C.M.; resources, A.L., P.S., G.T. and M.G.B.; data curation, G.M.S., G.A. and G.C.M.; writing—original draft preparation, G.M.S., G.T., L.B. and M.G.B.; writing—review and editing, P.S., G.C.M. and G.L.D.G.; visualization, G.M.S., G.A. and G.C.M.; supervision, G.T.; project administration, G.T., G.C.M. and M.G.B.; funding acquisition, G.T. and M.G.B. All authors have read and agreed to the published version of the manuscript.

Funding: The work reported in this publication was funded by the Italian Ministry of Health (RCR-2021-23671217 project, under the The Italian Musculoskeletal Apparatus Network RAMS) and by the 5xmille contributions to IRCCS Istituto Ortopedico Rizzoli (GAAC 2021/730563).

Institutional Review Board Statement: The present study was conducted in accordance with the Declaration of Helsinki, and the protocol was approved by the “Area Vasta Emilia Centro” Ethics Committee (CE-AVEC. Project identification code: Child-derot 718/2021/Oss/IOR).

Informed Consent Statement: Written informed consent has been obtained from the patient to publish this paper.

Data Availability Statement: The datasets generated during and/or analysed during the current study are available from the corresponding author on reasonable request.

Acknowledgments: We thank the Motion Laboratory Personnel of the Rizzoli Orthopaedic Institute for providing the gait analysis data used in this study.

Conflicts of Interest: The authors declare no conflict of interest.

References

- Kim, H.Y.; Cha, Y.H.; Chun, Y.S.; Shin, H.S. Correlation of the Torsion Values Measured by Rotational Profile, Kinematics, and CT Study in CP Patients. *Gait Posture* **2017**, *57*, 241–245. [[CrossRef](#)]
- O’Sullivan, R.; Walsh, M.; Jenkinson, A.; O’Brien, T. Factors Associated with Pelvic Retraction during Gait in Cerebral Palsy. *Gait Posture* **2007**, *25*, 425–431. [[CrossRef](#)]
- Chang, W.N.; Tsirikos, A.I.; Miller, F.; Schuyler, J.; Glutting, J. Impact of Changing Foot Progression Angle on Foot Pressure Measurement in Children with Neuromuscular Diseases. *Gait Posture* **2004**, *20*, 14–19. [[CrossRef](#)]
- Thielen, M.; Wolf, S.I.; Klotz, M.C.M.; Geisbüsch, A.; Putz, C.; Krautwurst, B.; Dreher, T. Supracondylar Femoral Rotation Osteotomy Affects Frontal Hip Kinetics in Children with Bilateral Cerebral Palsy. *Dev. Med. Child Neurol.* **2019**, *61*, 322–328. [[CrossRef](#)]
- Amirmudin, N.A.; Lavelle, G.; Theologis, T.; Thompson, N.; Ryan, J.M. Multilevel Surgery for Children With Cerebral Palsy: A Meta-analysis. *Pediatrics* **2019**, *143*, e20183390. [[CrossRef](#)]
- Lamberts, R.P.; Burger, M.; Du Toit, J.; Langerak, N.G. A Systematic Review of the Effects of Single-Event Multilevel Surgery on Gait Parameters in Children with Spastic Cerebral Palsy. *PLoS ONE* **2016**, *11*, e0164686. [[CrossRef](#)]
- McGinley, J.L.; Dobson, F.; Ganeshalingam, R.; Shore, B.J.; Rutz, E.; Graham, H.K. Single-Event Multilevel Surgery for Children with Cerebral Palsy: A Systematic Review. *Dev. Med. Child Neurol.* **2012**, *54*, 117–128. [[CrossRef](#)]
- Novak, I.; McIntyre, S.; Morgan, C.; Campbell, L.; Dark, L.; Morton, N.; Stumbles, E.; Wilson, S.A.; Goldsmith, S. A Systematic Review of Interventions for Children with Cerebral Palsy: State of the Evidence. *Dev. Med. Child Neurol.* **2013**, *55*, 885–910. [[CrossRef](#)]
- Sung, K.H.; Kwon, S.S.; Chung, C.Y.; Lee, K.M.; Cho, G.H.; Park, M.S. Long-Term Outcomes over 10 Years after Femoral Derotation Osteotomy in Ambulatory Children with Cerebral Palsy. *Gait Posture* **2018**, *64*, 119–125. [[CrossRef](#)]
- McCarthy, J.; Shrader, M.W.; Graham, K.; Veerkamp, M.; Brower, L.; Chambers, H.; Davids, J.R.; Kay, R.M.; Narayanan, U.; Novacheck, T.F.; et al. Establishing Surgical Indications for Hamstring Lengthening and Femoral Derotational Osteotomy in Ambulatory Children with Cerebral Palsy. *J. Child. Orthop.* **2020**, *14*, 50–57. [[CrossRef](#)]

11. Wren, T.A.L.; Lening, C.; Rethlefsen, S.A.; Kay, R.M. Impact of Gait Analysis on Correction of Excessive Hip Internal Rotation in Ambulatory Children with Cerebral Palsy: A Randomized Controlled Trial. *Dev. Med. Child Neurol.* **2013**, *55*, 919–925. [[CrossRef](#)]
12. Dugan, E.L.; Shilt, J.S. The Role of Motion Analysis in Surgical Planning for Gait Abnormalities in Cerebral Palsy. *Phys. Med. Rehabil. Clin. N. Am.* **2020**, *31*, 107–115. [[CrossRef](#)]
13. Benedetti, M.G.; Beghi, E.; De Tanti, A.; Cappozzo, A.; Basaglia, N.; Cutti, A.G.; Cereatti, A.; Stagni, R.; Verdini, F.; Manca, M.; et al. SIAMOC Position Paper on Gait Analysis in Clinical Practice: General Requirements, Methods and Appropriateness. Results of an Italian Consensus Conference. *Gait Posture* **2017**, *58*, 252–260. [[CrossRef](#)]
14. Baker, R.; Esquenazi, A.; Benedetti, M.G.; Desloovere, K. Gait Analysis: Clinical Facts. *Eur. J. Phys. Rehabil. Med.* **2016**, *52*, 560–574.
15. Klöpfer-Krämer, I.; Brand, A.; Wackerle, H.; Müßig, J.; Kröger, I.; Augat, P. Gait Analysis—Available Platforms for Outcome Assessment. *Injury* **2020**, *51*, S90–S96. [[CrossRef](#)]
16. Massaad, A.; Assi, A.; Bakouny, Z.; Sauret, C.; Khalil, N.; Skalli, W.; Ghanem, I. Three-Dimensional Evaluation of Skeletal Deformities of the Pelvis and Lower Limbs in Ambulant Children with Cerebral Palsy. *Gait Posture* **2016**, *49*, 102–107. [[CrossRef](#)]
17. Lofterød, B.; Terjesen, T.; Skaaret, I.; Huse, A.B.; Jahnsen, R. Preoperative Gait Analysis Has a Substantial Effect on Orthopedic Decision Making in Children with Cerebral Palsy: Comparison between Clinical Evaluation and Gait Analysis in 60 Patients. *Acta Orthop.* **2007**, *78*, 74–80. [[CrossRef](#)]
18. Ferrari, A.; Brunner, R.; Faccioli, S.; Reverberi, S.; Benedetti, M.G. Gait Analysis Contribution to Problems Identification and Surgical Planning in CP Patients: An Agreement Study. *Eur. J. Phys. Rehabil. Med.* **2015**, *51*, 39–48.
19. Sees, J.P.; Truong, W.H.; Novacheck, T.F.; Miller, F.; Georgiadis, A.G. What’s New in the Orthopaedic Treatment of Ambulatory Children with Cerebral Palsy Using Gait Analysis. *J. Pediatr. Orthop.* **2020**, *40*, E498–E503. [[CrossRef](#)]
20. Khouri, N.; Desailly, E. Contribution of Clinical Gait Analysis to Single-Event Multi-Level Surgery in Children with Cerebral Palsy. *Orthop. Traumatol. Surg. Res.* **2017**, *103*, S105–S111. [[CrossRef](#)]
21. Carty, C.P.; Walsh, H.P.J.; Gillett, J.G.; Phillips, T.; Edwards, J.M.; deLacy, M.; Boyd, R.N. The Effect of Femoral Derotation Osteotomy on Transverse Plane Hip and Pelvic Kinematics in Children with Cerebral Palsy: A Systematic Review and Meta-Analysis. *Gait Posture* **2014**, *40*, 333–340. [[CrossRef](#)]
22. Westberry, D.E.; Wack, L.I.; Davis, R.B.; Hardin, J.W. Femoral Anteversion Assessment: Comparison of Physical Examination, Gait Analysis, and EOS Biplanar Radiography. *Gait Posture* **2018**, *62*, 285–290. [[CrossRef](#)]
23. Bosmans, L.; Jansen, K.; Wesseling, M.; Molenaers, G.; Scheys, L.; Jonkers, I. The Role of Altered Proximal Femoral Geometry in Impaired Pelvis Stability and Hip Control during CP Gait: A Simulation Study. *Gait Posture* **2016**, *44*, 61–67. [[CrossRef](#)]
24. Scheys, L.; Desloovere, K.; Suetens, P.; Jonkers, I. Level of Subject-Specific Detail in Musculoskeletal Models Affects Hip Moment Arm Length Calculation during Gait in Pediatric Subjects with Increased Femoral Anteversion. *J. Biomech.* **2011**, *44*, 1346–1353. [[CrossRef](#)]
25. Scheys, L.; Desloovere, K.; Spaepen, A.; Suetens, P.; Jonkers, I. Calculating Gait Kinematics Using MR-Based Kinematic Models. *Gait Posture* **2011**, *33*, 158–164. [[CrossRef](#)]
26. Scheys, L.; Van Campenhout, A.; Spaepen, A.; Suetens, P.; Jonkers, I. Personalized MR-Based Musculoskeletal Models Compared to Rescaled Generic Models in the Presence of Increased Femoral Anteversion: Effect on Hip Moment Arm Lengths. *Gait Posture* **2008**, *28*, 358–365. [[CrossRef](#)]
27. Pitto, L.; Kainz, H.; Falisse, A.; Wesseling, M.; Van Rossom, S.; Hoang, H.; Papageorgiou, E.; Halleman, A.; Desloovere, K.; Molenaers, G.; et al. SimCP: A Simulation Platform to Predict Gait Performance Following Orthopedic Intervention in Children With Cerebral Palsy. *Front. Neurobot.* **2019**, *13*, 54. [[CrossRef](#)]
28. Galarraga, O.C.; Vigneron, V.; Khouri, N.; Dorizzi, B.; Desailly, E. Predictive Simulation of Surgery Effect on Cerebral Palsy Gait. *Comput. Methods Biomech. Biomed. Engin.* **2017**, *20*, 85–86. [[CrossRef](#)]
29. Frizziero, L.; Santi, G.M.; Liverani, A.; Napolitano, F.; Papaleo, P.; Maredi, E.; Di Gennaro, G.L.; Zarantonello, P.; Stallone, S.; Stilli, S.; et al. Computer-Aided Surgical Simulation for Correcting Complex Limb Deformities in Children. *Appl. Sci.* **2020**, *10*, 5181. [[CrossRef](#)]
30. Rajagopal, A.; Dembia, C.L.; DeMers, M.S.; Delp, D.D.; Hicks, J.L.; Delp, S.L. Full-Body Musculoskeletal Model for Muscle-Driven Simulation of Human Gait. *IEEE Trans. Biomed. Eng.* **2016**, *63*, 2068–2079. [[CrossRef](#)]
31. Leardini, A.; Sawacha, Z.; Paolini, G.; Ingrosso, S.; Nativio, R.; Benedetti, M.G. A New Anatomically Based Protocol for Gait Analysis in Children. *Gait Posture* **2007**, *26*, 560–571. [[CrossRef](#)] [[PubMed](#)]
32. Viceconti, M.; Taddei, F.; Montanari, L.; Testi, D.; Leardini, A.; Clapworthy, G.; Van Sint Jan, S. Multimod Data Manager: A Tool for Data Fusion. *Comput. Methods Programs Biomed.* **2007**, *87*, 148–159. [[CrossRef](#)] [[PubMed](#)]
33. Sholukha, V.; Leardini, A.; Salvia, P.; Rooze, M.; Van Sint Jan, S. Double-Step Registration of in Vivo Stereophotogrammetry with Both in Vitro 6-DOFs Electrogoniometry and CT Medical Imaging. *J. Biomech.* **2006**, *39*, 2087–2095. [[CrossRef](#)] [[PubMed](#)]
34. Thibault, J.B. Veo CT model-based iterative reconstruction. *GE Healthcare Chalfont St. Giles.* **2010**, 1–10.
35. Chiesa, A.M.; Spinnato, P.; Miceli, M.; Facchini, G. Radiologic Assessment of Osteosarcoma Lung Metastases: State of the Art and Recent Advances. *Cells* **2021**, *10*, 553. [[CrossRef](#)]
36. Osti, F.; Santi, G.M.; Neri, M.; Liverani, A.; Frizziero, L.; Stilli, S.; Maredi, E.; Zarantonello, P.; Gallone, G.; Stallone, S.; et al. CT Conversion Workflow for Intraoperative Usage of Bony Models: From DICOM Data to 3D Printed Models. *Appl. Sci.* **2019**, *9*, 708. [[CrossRef](#)]

37. Fedorov, A.; Beichel, R.; Kalpathy-Cramer, J.; Finet, J.; Fillion-Robin, J.C.; Pujol, S.; Bauer, C.; Jennings, D.; Fennessy, F.; Sonka, M.; et al. 3D Slicer as an Image Computing Platform for the Quantitative Imaging Network. *Magn. Reson. Imaging* **2012**, *30*, 1323–1341. [[CrossRef](#)]
38. Blender.com Blender.Org—Home of the Blender Project—Free and Open 3D Creation Software. Available online: <https://www.blender.org/> (accessed on 2 August 2022).
39. MeshLab. Available online: <https://www.meshlab.net/> (accessed on 2 August 2022).
40. Napolitano, F.; Frizziero, L.; Santi, G.M.; Donnici, G.; Liverani, A.; Papaleo, P.; Giuseppetti, V. Description of the Cad-Am Process for 3d Bone Printing: The Case Study of a Flat Foot. In Proceedings of the 5th NA International Conference on Industrial Engineering and Operations, Detroit, MI, USA, 10–14 August 2020.
41. Valente, G.; Crimi, G.; Vanella, N.; Schileo, E.; Taddei, F. NMSBUILDER: Freeware to Create Subject-Specific Musculoskeletal Models for OpenSim. *Comput. Methods Programs Biomed.* **2017**, *152*, 85–92. [[CrossRef](#)]
42. Bakhshayesh, P.; Sandberg, O.; Kumar, V.; Ali, A.; Enocson, A. Volume Fusion of CT Images to Measure Femoral Symmetry. *Surg. Radiol. Anat.* **2020**, *42*, 635–639. [[CrossRef](#)]
43. Zeng, C.; Xing, W.; Wu, Z.; Huang, H.; Huang, W. A Combination of Three-Dimensional Printing and Computer-Assisted Virtual Surgical Procedure for Preoperative Planning of Acetabular Fracture Reduction. *Injury* **2016**, *47*, 2223–2227. [[CrossRef](#)]
44. Shen, S.; Wang, P.Z.; Li, X.Y.; Han, X.; Tan, H.L. Pre-Operative Simulation Using a Three-Dimensional Printing Model for Surgical Treatment of Old and Complex Tibial Plateau Fractures. *Sci. Rep.* **2020**, *10*, 6044. [[CrossRef](#)]
45. Frizziero, L.; Santi, G.M.; Liverani, A.; Giuseppetti, V.; Trisolino, G.; Maredi, E.; Stilli, S. Paediatric Orthopaedic Surgery with 3D Printing: Improvements and Cost Reduction. *Symmetry* **2019**, *11*, 1317. [[CrossRef](#)]
46. Ravera, E.P.; Crespo, M.J.; Catalfamo Formento, P.A. A Subject-Specific Integrative Biomechanical Framework of the Pelvis for Gait Analysis. *Proc. Inst. Mech. Eng. Part H J. Eng. Med.* **2018**, *232*, 1083–1097. [[CrossRef](#)]
47. Alrehily, F.; Hogg, P.; Twiste, M.; Johansen, S.; Tootell, A. Scoliosis Imaging: An Analysis of Radiation Risk in the CT Scan Projection Radiograph and a Comparison with Projection Radiography and EOS. *Radiography* **2019**, *25*, e68–e74. [[CrossRef](#)]
48. Roskopf, A.B.; Ramseier, L.E.; Sutter, R.; Pfirrmann, C.W.A.; Buck, F.M. Femoral and Tibial Torsion Measurement in Children and Adolescents: Comparison of 3D Models Based on Low-Dose Biplanar Radiography and Low-Dose CT. *Am. J. Roentgenol.* **2014**, *202*, W285–W291. [[CrossRef](#)]
49. Escott, B.G.; Ravi, B.; Weathermon, A.C.; Acharya, J.; Gordon, C.L.; Babyn, P.S.; Kelley, S.P.; Narayanan, U. EOS Low-Dose Radiography: A Reliable and Accurate Upright Assessment of Lower-Limb Lengths. *J. Bone Jt. Surg.* **2013**, *95*, e183. [[CrossRef](#)]
50. Altahawi, F.; Pierce, J.; Aslan, M.; Li, X.; Winalski, C.S.; Subhas, N. 3D MRI of the Knee. *Semin. Musculoskelet. Radiol.* **2021**, *25*, 455–467. [[CrossRef](#)]
51. MSMS Software Downloads—USC Viterbi | Department of Biomedical Engineering. Available online: <https://bme.usc.edu/msms-software-downloads/> (accessed on 2 August 2022).
52. Cleather, D.J.; Bull, A.M.J. The Development of a Segment-Based Musculoskeletal Model of the Lower Limb: Introducing FREEBODY. *R. Soc. Open Sci.* **2015**, *2*, 140449. [[CrossRef](#)]